PAPERmaking!
FROM THE PUBLISHERS OF PAPER TECHNOLOGY
Volume 5, Number 2, 2019

Paper Industry Technical Association

Effects of rotational velocity and hold time at folding posture on time-dependent release behavior of creased white-coated paperboard

Shigeru NAGASAWA, Satoshi KANEKO and Dai ADACHI

In this work, a folding experiment was performed to investigate the time-dependent creasing characteristics of white-coated paperboard of 0.3mm thickness. After folding up to the tracking angle of 90° under a specified rotational velocity, the creased part was held for a chosen short time (0~20s) and the time-dependent release behavior of folding angle was experimentally investigated for the elapsed release time of 10s. When using the paperboard scored with a specified indentation depth, both the hold time of folded posture of creased part and the rotational velocity of fixture were varied. The folding angle of the paperboard was measured by a CCD camera of digital microscope and the bending moment resistance was measured by a load cell of bending test apparatus in the folding experiment. Through the experiment, it was found that the time-dependent release angle consisted of the hold time based intercept part and the creep-recovery based gradient part as a logarithmic function of the elapsed release time. When varying the folding velocity against a fixed unfolding velocity, the unfolded released behavior was isolated by the hold time from the first half folding velocity. Seeing the drop rate of bending moment at the tracking position and the dependency of initial release angle on the rotational velocity, a transient state and quasi-stationary state of bending moment relaxation were revealed.

Contact information:
Department of Mechanical Engineering, Nagaoka University of Technology 1603-1 Kamitomioka-machi, Nagaoka-shi, Niigata 940-2188, Japan

Journal of Advanced Mechanical Design, Systems, and Manufacturing, Vol.13, No.1 (2019), Paper No.18-00230 [DOI: 10.1299/jamdsm.2019jamdsm0004]

Bulletin of the JSME Vol.13, No.1, 2019
Journal of Advanced Mechanical Design, Systems, and Manufacturing

Effects of rotational velocity and hold time at folding posture on time-dependent release behavior of creased white-coated paperboard

Shigeru NAGASAWA*, Satoshi KANEKO* and Dai ADACHI*
* Department of Mechanical Engineering, Nagaoka University of Technology
1603-1 Kamitomioka-machi, Nagaoka-shi, Niigata 940-2188, Japan
E-mail: snaga@mech.nagaokaut.ac.jp

Received: 6 May 2018; Revised: 24 November 2018; Accepted: 17 December 2018

Abstract
In this work, a folding experiment was performed to investigate the time-dependent creasing characteristics of white-coated paperboard of 0.3mm thickness. After folding up to the tracking angle of 90° under a specified rotational velocity, the creased part was hold for a chosen short time (0~20s) and the time-dependent release behavior of folding angle was experimentally investigated for the elapsed release time of 10s. When using the paperboard scored with a specified indentation depth, both the hold time of folded posture of creased part and the rotational velocity of fixture were varied. The folding angle of the paperboard was measured by a CCD camera of digital microscope and the bending moment resistance was measured by a load cell of bending test apparatus in the folding experiment. Through the experiment, it was found that the time-dependent release angle consisted of the hold time based intercept part and the creep-recovery based gradient part as a logarithmic function of the elapsed release time. When varying the folding velocity against a fixed unfolding velocity, the unfolded released behavior was isolated by the hold time from the first half folding velocity. Seeing the drop rate of bending moment at the tracking position and the dependency of initial release angle on the rotational velocity, a transient state and quasi-stationary state of bending moment relaxation were revealed.

Keywords : Folding, Shear, Bending moment, Creasing, Relaxation, Creep, Paperboard

1. Introduction

Coated paperboard is a fundamental raw material for various printed-decorated packaging and transport packaging industries due to its advantages such as high strength-to-weight ratio, high surface smoothness, printability, sustainability, recyclability (Kirwan, 2013). If any cracks occur on the outside of the folded parts of paperboard, which is used for making a cabinet, the mechanical strength of the cabinet is weakened and also the folded parts are inferior in decorative aspects. Actual creasing range was investigated based on the relationship between the crease depth and crease width by Hine (1959). Nagasawa et al. (2003; 2008; 2011) reported about the quasi-static folding stiffness with respect to the indentation depth of the creaser and also discussed about the crease deviation effect on the folding deformation characteristics. Also, several advanced results are reported for the de-lamination mechanism and bulging deformation considering anisotropic material properties (Beex, et al., 2009; Nygards, et al., 2009; Sudo, et al., 2005). However, they were mainly based on the quasi-static solid mechanics.

On the other hands, the time-dependent bending moment resistance acting on a hinge which is folded onto a scored line, is important in order to adjust the mechanical conditions of boxing stage performed by an automatic folder gluer. Various time-dependent problems on actual deformation phenomenon have not been sufficiently discussed in the past, although there are several reports of fiber creep and in-plane tensile relaxation of thin paper (Johanson et al., 1964; Sharon, et al., 2010). It is difficult to estimate various time-dependent responses from the quasi-static strength of a creased part, such as the maximum bending moment and the initial gradient of bending moment. Since such the transient deformation of the creased part subjected to a bending moment was not observed by any movie camera or load cells during the dynamic bending test, the time-dependent bending stiffness or its residual strain state could not be verified

Paper No.18-00230
[DOI: 10.1299/jamdsm.2019jamdsm0004]

directly while the quasi-static bending was examined (Nagasawa, et al., 2014). Recently, Nagasawa et al. investigated the relaxation characteristics of bending moment resistance of 0.3 mm thickness white-coated paperboard during a folding motion from an initial position up to various tracking angles, and through the bending test by the use of the bending moment measurement apparatus (CST-J-1, 2013), the relaxation of the bending moment resistance was investigated by an exponential coefficient of logarithmic function which was independent to the normalized indentation depth and the tracking angle (Nagasawa, et al., 2014; 2015). Furthermore, a creep-recovery (release) response of folded angle during returning back was also approximated by a logarithmic function of elapsed time. Seeing the effect of rotational velocity on the release angle when the holding (stopping) time was kept in 0s at the tracking position, the initial release angle decreased with the rotational velocity (Nagasawa, et al., 2016). Here, the initial release angle was determined at the time when the reaction force of folding becomes zero. However, in that report, the effect of holding (stopping) time at the tracking position on the released behavior was not discussed. Therefore, the combination effect of the rotational velocity during folding/unfolding process and the hold time at the tracking position on the release behavior was investigated in this work. Firstly, the time-dependent behavior of release angle was reviewed under the specified rotational velocity of fixture 0.2 rps (revolution per second) (1.26 rad·s^{-1}) when varying the hold time, and some coefficients of logarithmic approximation of release angle was discussed. Secondly, the initial released angle (when the rotation force of folding becomes zero) was investigated when both the rotational velocity and the holding (stopping) time were varied in a certain range.

2. Experimental condition and method

2.1 Initial creasing of specimen for pre-processing

Figure 1 illustrates viewpoints of a paperboard. The prepared white-clay-coated paperboard (basis weight ρ=228~237 g·m^{-2}) had a thickness of t=0.3 (0.297~0.303) mm. Table 1 shows the analysis result of fiber size and pulp combination ratio. Regarding the mechanical properties of the paperboard, the in-plane tensile test properties in the Machine Direction of paper making (MD, the principal axis direction with reference to the fiber grain direction), were shown in Table 2. The specimens were kept in a room which had a temperature of 296 K and a humidity of 50 %RH. The test pieces were prepared as 5 pieces of rectangle-shaped white-coated paperboard, which had a width of 15 mm, length of 60 mm, for each condition.

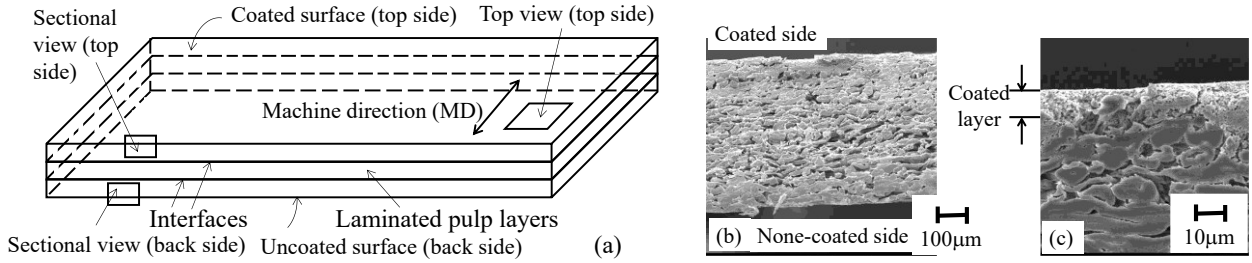

Figure 1 Outline of coated paperboard. (a) Schematic illustration. (b) SEM sectional view. (c) Top side SEM sectional view. The paperboard is composed of multiple plies and the coated top layer and the uncoated back layer are generally different (strong or tough) from the middle layer. When scoring the out-of-plane (top or back side) by the use of round-edge punching tool, the bonded interfaces of pulp layers apt to be de-laminated. This de-lamination is used for folding the paperboard without any breaking of outside layers.

Table 1 Size of fiber and pulp combination ratio of coated paperboard 230 (measured by Kajaani-FS300) L-BKP: Broad-leaved lumber (hard wood), bleaching kraft pulp; N-BKP: Needle-leaved lumber (soft wood), bleaching kraft pulp; N-TMP: Needle-leaved, thermal mechanical pulp; L(n): based on number of fibers in each fibrillation index class; L(l): based on length weighted number of fibers in each fibrillation index class; L(w): based on weight-weighted number of fibers in each fibrillation index class; CWT: Wall thickness of cell; Width: average width of fiber.

Unit	Pulp combination ratio /%			Projected length of fiber /mm			Size /μm		Section area /μm^2
Item	L-BKP	N-BKP	N-TMP	L(n)	L(l)	L(w)	Width	CWT	CSA
Value	83.1	16.9	0.0	0.45	0.88	1.36	18.2	4.6	206.2

[DOI: 10.1299/jamdsm.2019jamdsm0004]

In order to make a smooth folding, a paperboard is usually scored by using a creaser at the pre-stage and make a localized delamination. (Kirwan, 2005). When the creased part is folded, the topside layers of fiber on the coated side are extended and require an adequate tensile strength and stretch, while the backside layers are compressed and bulged. In order to make a smart folding under forming the bulged zone, a scoring is processed before folding the paperboard.

Table 2 In-Plane tensile properties of white-coated paperboard in Machine direction (MD). Tensile feed velocity was 0.33 mm·s^{-1} (strain rate: 0.00183 s^{-1}). Based on the procedure of JIS-P8113.

Ultimate Tensile Strength	σ_B MPa	41.1 (40.2~42.7)
Breaking true strain	ε_B %	1.71 (1.62~1.81)
Young's modulus	E GPa	5.72 (5.53~5.91)

The specimen was scored using a round-edge knife (a creaser) and rubber blocks as shown in Fig.2. Here, the creaser was set across MD of the specimen. Figure 3 shows a scoring state (crease forming) of a paperboard specimen using the creaser with a radius of r= 0.355 mm, thickness of b=0.71 mm. When the creaser is indented to the paperboard, the expression: tan $\delta = (2d \cdot B^{-1}) = \gamma$ is the average shearing strain. This quantity γ is defined as the normalized indentation depth (Nagasawa et al., 2001). Also, using the paperboard thickness t and the thickness of creaser b, the groove width B was empirically chosen as $2t+b$ = 1.3 mm, the height of groove H was 1.5mm and the indentation of creaser d was chosen as $d < H$. Regarding the time-dependent response of bending moment resistance (Nagasawa et al., 2014, 2015), the scored state of crease part was investigated as γ= 0.2~1.0, while the previous work (Nagasawa, et al., 2016) mainly discussed with the scored state of γ= 0.6. This was also chosen here owing that the indentation depth was empirically designed as γ= 0.4~0.6 ($d \approx t$). The scoring condition (using a rubber height of 7 mm by the hardness of 40(A) and a creaser height of 5.6 mm) was empirically chosen from a commercial based production. All the specimens were formed without warpages. The feed velocity of creaser was chosen as V = 0.0167 mm·s^{-1} for scoring.

2.2 Folding and release of scored specimen

Figure 4 illustrates a conceptual mechanism of crease folding. When the paperboard is scored by a creasing knife, the intermediate layers are damaged as shown in Fig.4(a). Since the paperboard consisted of laminated plies, a certain extent of de-lamination damage is generated in the scored zone. When the paperboard is folded with this scored position, the damaged layers are further de-laminated and its inside (lower) layers are bulged as shown in Fig.4(b) (Hine, 1959; Nagasawa, 2004). The bending moment resistance of the creased zone appeared to consist of three mechanisms: (i) a tensile resistance of the outside (upper) layers, (ii) a compressive resistance of the inside (lower) layers, and (iii) a detaching (peeling) resistance of the middle layers (Nagasawa et al., 2011). The third item (detaching) affects only the transient folding resistance in the early stage, while the first (tensile of outside) and second (compression of bulged layers) items behave as the bending moment resistance in the full stage of folding test. Figure 5 shows a general view of bending test apparatus (CST-J-1, 2003). Figure 6 shows a conceptual illustration of the folding process and rotating method used in the bending test.

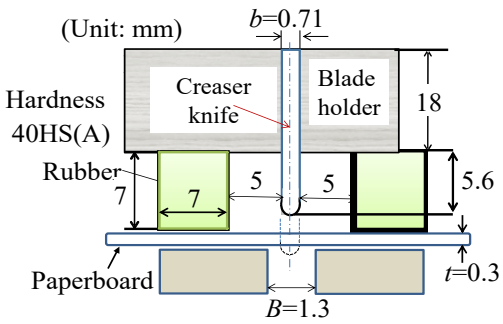

Figure 2 Layout of out-of-plane scoring by creaser

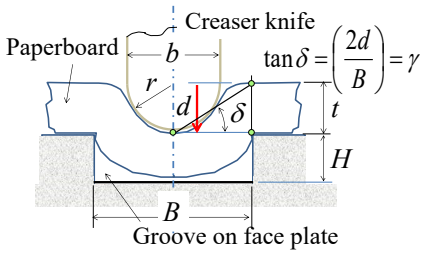

Figure 3 Schematic of scoring state and parameters

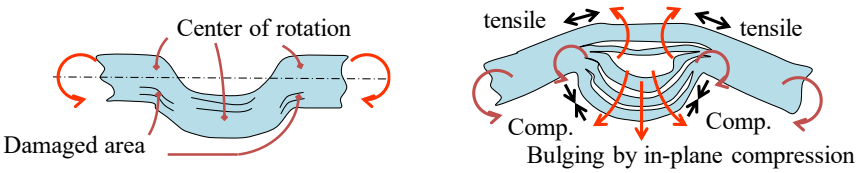

(a) Concave shape after scoring (b) Behavior of crease in folding process

Figure 4 Model of crease mechanism. (a) Scoring by creaser knife makes damaged area in a laminated paperboard, and causes an offset with the center position of rotation. (b) Lateral in-plane compression on the inside layer buckles and makes the inside layer bulged. This moves the neutral plane of bending upwards and reduces the tensile stress in the outside layer. (Ref. Nagasawa, S. et al., 2004)

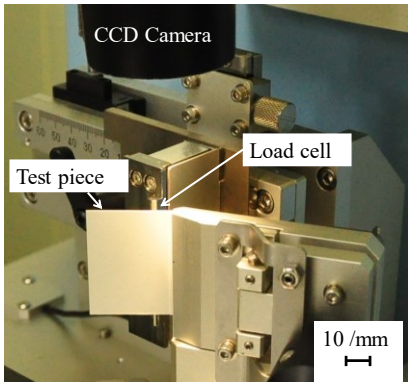

Figure 5 General view of bending test apparatus

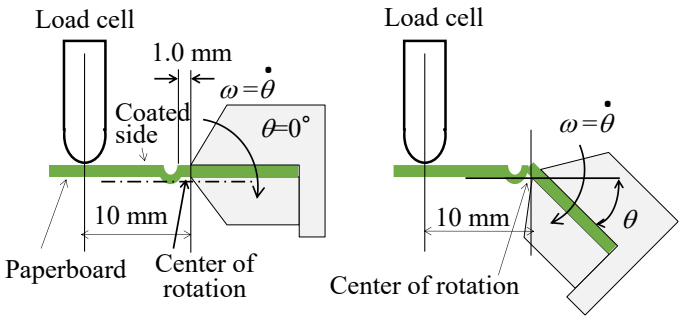

Figure 6 Conception of bending test (folding process)

In the folding process, the folding angle θ was recorded by a CCD camera of digital microscope, while the bending moment M was measured by a load cell of the bending test apparatus. A scored paperboard was set up in the test apparatus and clamped by the fixture which rotated with the rotational velocity ω. The clamping position was shown in Fig.6. The scored paperboard was bent from the original position $\theta = 0°$ up to the folding angle of $\theta = 90°$. The folding process was completed at 90° (named as the tracking angle $\Theta = 90°$) and its angle of fold state was paused for a specified duration defined as the elapsed hold (stopping) time t_{1ep}. This pause of Θ=90° was used for observing the relaxation of bending moment. After completing this relaxation process with the hold time t_{1ep}, the folded paperboard is sequentially released under returning back with the unfolding rotational velocity ω' until the reaction force of the load cell becomes zero. This returning back duration was named as the unfolding or release process.

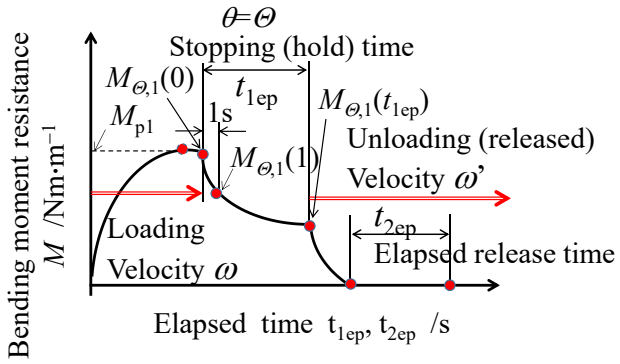

Figure 7 Conceptual bending moment response with elapsed time and measured parameters.

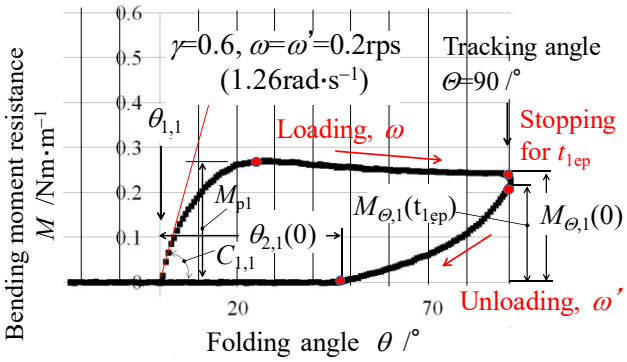

Figure 8 Analysis parameters on folding resistance diagram.

The conceptual relationship between the bending moment resistance (for the unit width) M and the elapsed time was illustrated in Fig.7. Figure 8 is an example of the first round's folding load response described as the relationship between the folding rotation angle θ and bending moment resistance M. The first term maximum peak bending moment M_{p1} and the bending moment at the first round's tracking angle $M_{\Theta(=90°),1}(t_{1ep})$ were explained in the previous report

[DOI: 10.1299/jamdsm.2019jamdsm0004]

(Nagasawa et al., 2014, 2015). The first round's starting angle $\theta_{1,1}$ was zero (in a flat attitude). In this work, only the first round was considered (the number of folding repetition was suffixed as ",1"). The early stage in which θ was less than 20° was mainly characterized by the elastic bending stiffness without detaching and bulging of inside layers. Since the middle stage (20° <θ< 90°) had a certain stationary resistance (almost constant) under the specified rotation velocity ω, the behavior of resistance appeared to be a sort of the creep response of Maxwell type two-element model (Betten, 2002).

This bending moment diagram was used here for confirming the hold time t_{1ep} =0~20s and detecting the initial unfolded state t_{2ep}=0s. Here, t_{2ep} is the elapsed release time for observing the release angle $\theta_{2,1}$. The quantity $\theta_{2,1}(0)$ is the initial release angle.

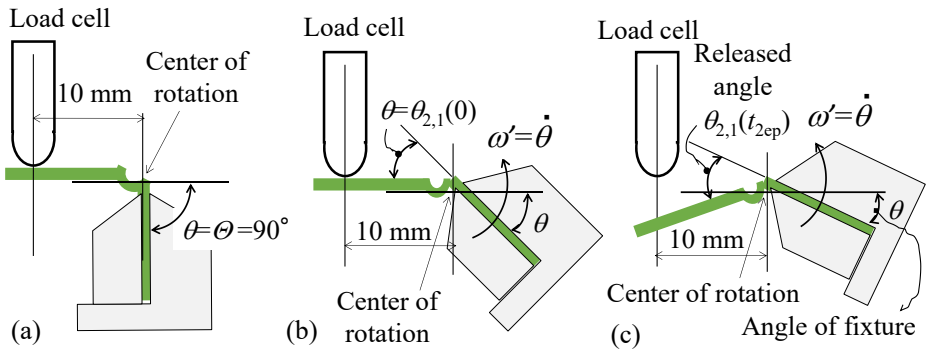

Figure 9 Schematics of unfolding and relationship between release angle and fixture angle (a) State of tracking angle of 90°; (b) State of initial release angle (t_{2ep}=0) when reaction force of load cell becomes zero; (c) In case of unfolded state when detaching the load cell (for t_{2ep}>0).

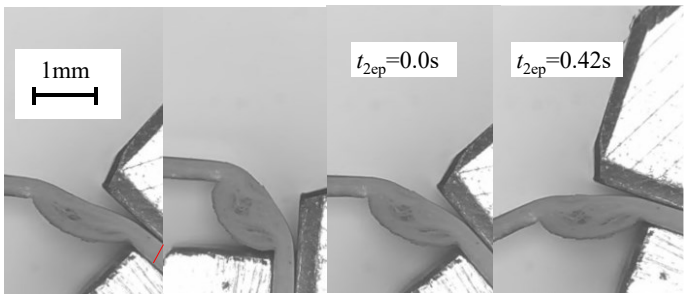

(a) θ=34.0° (b) θ=89.9° (c) $\theta=\theta_{2,1}$=46.0° (d) $\theta_{2,1}$=42.7°

Figure 10 CCD camera photographs of side views of creased part during folding test (γ=0.6, ω=0.2 rps). (Ref. Nagasawa, S. et al., 2016)

Figure 9 illustrates three states of unfolding process: (a) the state of tracking angle of Θ = 90°, (b) the initial released state when defining t_{2ep}=0, and (c) the released state after detaching the load cell. Generally, $\theta_{2,1}$ is not equal to the rotation angle of fixture θ for t_{2ep}>0, while $\theta_{2,1}$ is equal to θ at t_{2ep}=0 or before detaching the load cell. Figure 10 showed representative side views of real creased part during a folding test. In the folding process (a),(b), the bulged inside layers were compressed in the in-plane direction, while the height of bulged zone decreased with the released angle $\theta_{2,1}$ in the unfolding process (c),(d). Namely, the released behavior of folded attitude appeared to be mainly caused by the released energy of compressed and bulged layers.

According to the preliminary experiments (Nagasawa, et al., 2014, 2015), the relationship between the bending moment at the tracking position $M_{\Theta(=90°),1}$ and the hold time t_{1ep} was linearly approximated with the logarithmic term $\ln(t_{1ep})$ using Eq.(1),(2). Here, the intercept a_0 was defined as $M_{90,1}(1)$ (at t_{1ep}=1s), a_1 was the gradient coefficient of Eq.(1), and the exponential coefficient p_1 of relaxation was defined as the ratio of a_1/a_0. They describe the relaxation characteristics of bending moment accumulated at the tracking angle of 90°.

$$M_{90,1} = -a_1 \ln(t_{1ep}) + a_0 \quad (1)$$

$$M_{90,1}/a_0 = \bar{M}_{90,1} = 1 - p_1 \ln(t_{1ep}), \qquad p_1 = a_1/a_0 \quad (2)$$

The logarithmic relaxation of bending moment at the holding of θ=90° was similar to the stress relaxation of the white-coated paperboard subjected to an uni-axial tensile displacement (Nagasawa et al., 2017). Namely, the value of

[DOI: 10.1299/jamdsm.2019jamdsm0004]

exponential coefficient p_1 of bending resistance was almost equal to that of uni-axial tensile displacement. This means that the tensile relaxation of in-plane direction is a major factor in the bending resistance.

Regarding the relationship between the release angle $\theta_{2,1}$ and the elapsed release time t_{2ep}, the linear approximation with the logarithmic term $\ln(t_{2ep})$ was introduced (Nagasawa, et al., 2016) as Eq.(3),(4). Here, the intercept b_0 was defined as $\theta_{2,1}(1)$ (at t_{2ep}=1s), b_1 was the gradient coefficient of Eq.(3), and the exponential coefficient p_2 was defined as the ratio of b_1/b_0. They describe the creep-recovery characteristics of folded angle.

$$\theta_{2,1} = -b_1 \ln(t_{2ep}) + b_0 \tag{3}$$

$$\theta_{2,1}/b_0 = \bar{\theta}_{2,1} = 1 - p_2 \ln(t_{2ep}), \qquad p_2 = b_1/b_0 \tag{4}$$

Since the transient response seems to be caused by the relaxation and creep-recovery characteristics of paperboard during the folding process, the effect of fixture's rotational velocity ω (folding) and ω' (unfolding) on the release angle $\theta_{2,1}(t_{2ep})$ was investigated for the range of t_{2ep}=0~10s when γ = 0.6.

The synchronized condition of ω=ω' was mainly investigated and its value was chosen as 0.02, 0.03, 0.05, 0.1, 0.2, 0.3 and 0.4 rps (0.13, 0.19, 0.31, 0.63, 1.26, 1.88, 2.51 rad·s^{-1}). For the sake of comparison of asynchronous condition, when the returning back velocity was chosen as a constant of ω'=0.2 rps (1.26 rad·s^{-1}), the folding velocity ω was chosen as 0.02, 0.03, 0.05, 0.1, 0.2, 0.3 and 0.4 rps (0.13, 0.19, 0.31, 0.63, 1.26, 1.88, 2.51 rad·s^{-1}).

3. Results and discussion

3.1 Response of bending moment with rotational velocity

In the synchronized condition of ω=ω'= 0.2 rps (1.26 rad·s^{-1}), Fig.8 illustrated a representative case of bending moment resistance M with the folding angle θ. Since the intermediate stage (20°<θ<90°) appeared to be a sort of creep response of Maxwell type two-element model in Fig.8, the values of M_{p1} and $M_{90,1}(0)$ were expected to increase with ω. When varying the velocity ω (= ω'), the maximum peak bending moment M_{p1}, and the relaxed bending moment at t_{1ep}= 0s, 1s with Θ= 90°: $M_{90,1}(0)$, $M_{90,1}(1)$ were measured and shown in Fig.11. Eq. (5), (6), (7) were derived as linear approximations with the logarithmic term $\ln(\omega/0.2)$ from the experimental result.

$$M_{p1} = 0.013 \ln(\omega/0.2) + 0.244 \tag{5}$$

$$M_{90,1}(0) = 0.0061 \ln(\omega/0.2) + 0.215 \tag{6}$$

$$M_{90,1}(1) = a_0 = -0.004 \ln(\omega/0.2) + 0.175 \tag{7}$$

Seeing Eq.(5),(6), the bending moment under the folding process increased with the rotational velocity ω (= ω'). This tendency matched the prediction of Maxwell type relaxation response. However, the relaxed bending moment $M_{90,1}(1)$ decreased with ω (= ω') from Eq. (7). This means that the dissipation energy or the bending moment drop increases with the rotational velocity ω for a short duration t_{ep1}<1s.

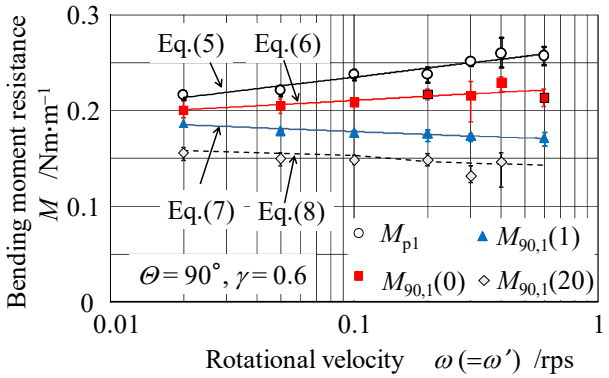

Figure 11 Dependency of bending moment on rotational velocity. The unfolding velocity ω' was equal to the folding velocity ω. As the representative quantities of bending moment resistance, the maximum peak M_{p1}, the relaxed three states at the tracking position $M_{90,1}(0)$, $M_{90,1}(1)$ and $M_{90,1}(20)$ were plotted as the average (with the maximum and minimum bar).

Seeing the preliminary experiment (Nagasawa, et al., 2015, Fig.14), since the exponential coefficient of relaxation p_1

[DOI: 10.1299/jamdsm.2019jamdsm0004]

was expressed with $\omega/0.2$ for $0.2<\omega/0.2<3$, the relaxed bending moment at t_{1ep}=20s was estimated using Eq.(8). Here, a_0 was calculated from Eq.(7), and p_1 was estimated as 0.046 for $\omega/0.2<0.5$ and 0.055~0.057 for $0.5<\omega/0.2<3$ from the preliminary experiment. The result of Eq.(8) was well similar to the current experiment as shown in Fig.11.

$$M_{90,1}(t_{1ep}) = a_0 (1-p_1 \ln(t_{1ep})) \tag{8}$$

So far, it was revealed that the bending moment at the pre-stage of tracking position (Θ=90°) was sufficiently accumulated as an elastic strain energy, namely the measured quantities M_{p1} and $M_{90,1}(0)$ increased with the folding velocity ω, whereas the quasi-stationary relaxation of the bending moment was performed when the hold time was kept in a certain duration. In such the relaxation state based on the hold time (t_{1ep}> 1s), the bending moment decreased slightly with ω. Also, a drop rate of the bending moment in the early stage of holding process increased with ω, owing that the difference of Eq.(6) and Eq.(7) derived the drop rate $M_{90,1}(0)-M_{90,1}(1)= 0.01 \ln(\omega/0.2) + 0.04$.

3.2 Dependency of release angle on hold time

Figure 12 (a) shows a relationship between the first round's release angle $\theta_{2,1}$ and the elapsed release time t_{2ep} when choosing the hold time t_{1ep} as 0, 5, 10 and 20s under the synchronized condition $\omega=\omega'$=0.2 rps (1.26 rad·s^{-1}). Here, the value of $\theta_{2,1}$ was plotted as the average of 5 samples. Seeing Figure 12 (a), it is found that the variation of $\theta_{2,1}$ is decreased as a logarithmic form with t_{2ep}, and the intercept of $\theta_{2,1}(1)$ tends to be increased with t_{1ep}. Hence, the release angle $\theta_{2,1}$ was approximated with the term $\ln(t_{2ep})$ using Eq.(3), (4).

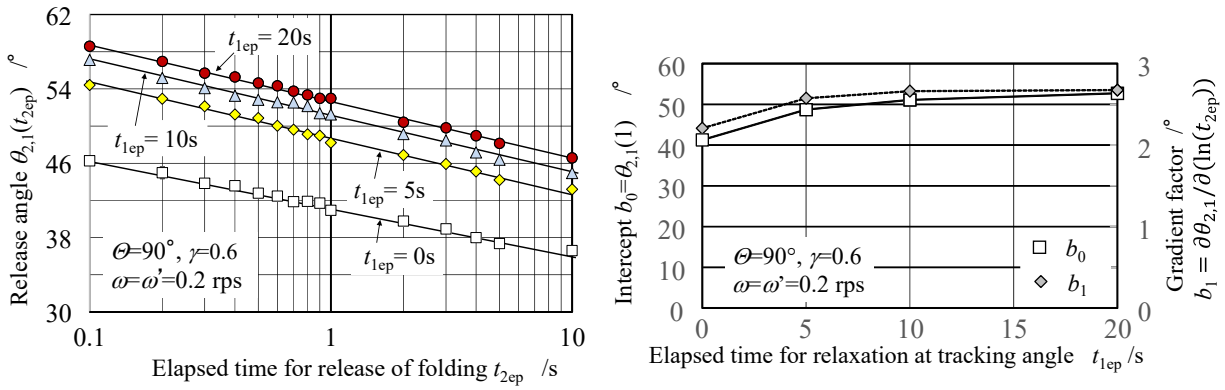

(a) Relationship between release angle (average) and elapsed release time when varying hold time

(b) Approximation coefficients of folding angle of crease with respect to hold time

Figure 12 Response of release angle (average) with respect to elapsed release time when keeping rotational velocity $\omega=\omega'$=0.2 rps (1.26 rad·s^{-1}). The standard deviation of measured release angle was about 0.7°.

Figure 12 (b) arranges the dependency of those two coefficients b_1, b_0 on the hold time t_{1ep}. It is found that the intercept b_0 is remarkably varied in a short time less than 5s, while it tends to be saturated or asymptotically increased for t_{1ep} >5s. Since the exponent coefficient p_2 was about 0.050~0.053 in stable, the time-delay characteristic (creep-recovery) of release angle appears to be independent to the hold time, when keeping $\omega=\omega'$=0.2 rps (1.26 rad·s^{-1}).

3.3 Dependency of initial release angle on rotational velocity

According to the preliminary experiment (Nagasawa et al., (2016), Fig.15), when ω> 0.1 rps (0.63 rad·s^{-1}) and t_{1ep} = 0s, the exponential coefficient p_2 was about 0.05 for t_{2ep} =0.2~10s, namely p_2 appeared to be insensitive for ω>0.1 rps (0.63 rad·s^{-1}). Since the expression of Eq.(4) is composed of two factors p_2 and b_0, in order to discuss the effect of hold time on the release angle, the behavior of the intercept $b_0 = \theta_{2,1}(1)$ seems to be necessary. In this work, the initial release angle $\theta_{2,1}(0)$ was measured and analyzed instead of $\theta_{2,1}(1)$.

Figure 13 shows the initial release angle $\theta_{2,1}(0)$ when varying the hold time t_{1ep}= 0~20s at the tracking angle Θ=90°. Here, the synchronized condition was considered: $\omega=\omega'$ = 0.02~0.4rps (0.13~2.51rad·s^{-1}). The value $\theta_{2,1}(0)$ was the average of 5 samples and the error bar shows the maximum and minimum value in the 5 samples for each rotational velocity. It is found that $\theta_{2,1}(0)$ tends to be linearly varied with a logarithmic function of rotational velocity.

Therefore, Eq.(9) was introduced and the gradient coefficient β_1 and the intercept $\beta_0 = \theta_{2,1}(0)|_{\omega=0.2rps}$ were investigated

[DOI: 10.1299/jamdsm.2019jamdsm0004]

and arranged in Fig. 14.

$$\theta_{2,1}(0)= \beta_1 \ln(\omega / 0.2) + \beta_0 , \quad \beta_0= \theta_{2,1}(0)|_{\omega=0.2\text{rps}} \tag{9}$$

Seeing Figure 13 and Fig.14, the gradient β_1 was changed from the negative (decrease) to the positive (increase) in a short time holding: 1s<t_{1ep}<2s. It was asymptotically and slightly increased for t_{1ep} >5s. This tendency seems to be caused by the relaxation of folding posture against the pre-stage accumulation of elastic bending energy. If the hold time is sufficiently long for reducing the residual bending stress, the effect of folding (first half) rotational velocity ω seems to be isolated and then only the unfolding (second half as the returning back) velocity ω' appears to affect the initial release angle.

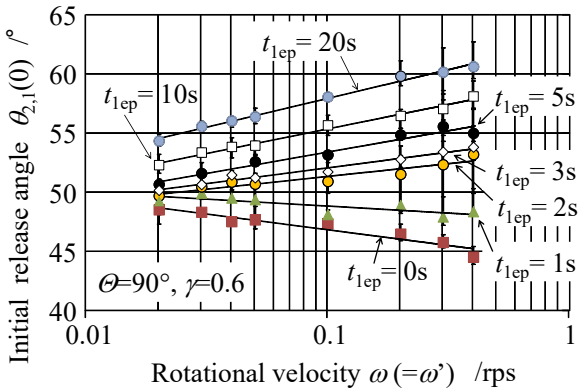

Figure 13 Relationship between initial released angle and synchronized rotational velocity by varying hold time.

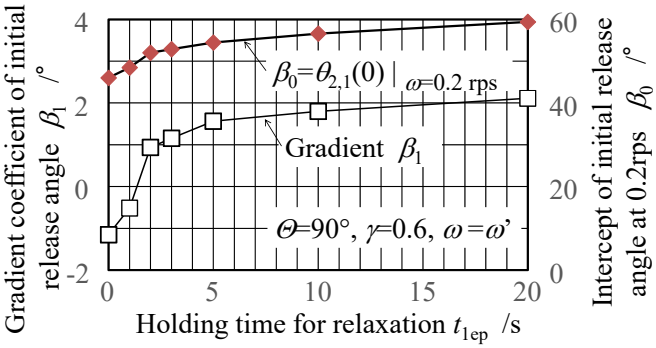

Figure 14 Gradient and intercept of initial released angle with respect to rotational velocity when varying hold time.

In order to verify this isolation effect, an additional experiment was carried out. Namely, when the unfolding velocity was kept in ω'= 0.2 rps (1.26 rad·s^{-1}), the folding velocity ω was chosen as 0.02, 0.2 and 0.4 rps (0.13, 1.26, 2.51 rad·s^{-1}). This is the asynchronous condition. Figure 15 shows a ratio of the coefficients of Eq.(9): β_1/β_0 with respect to the hold time t_{1ep} =0~20s. Here, the synchronized condition (ω=ω') was derived from Fig.14. It is found that the coefficient ratio of asynchronous condition is sufficiently small-positive for t_{1ep}>10s. The effect of first half rotational velocity ω is fairly isolated by the hold time of 10~20s, but its effect is observed in a small extent.

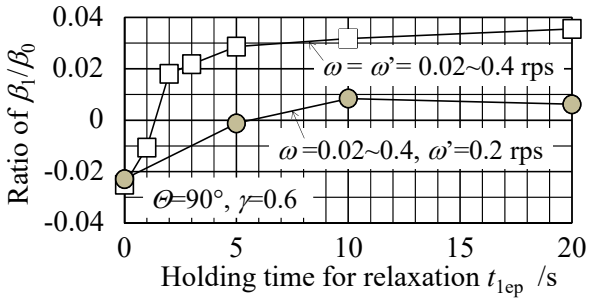

Figure 15 Comparison of ratio of coefficients β_1/β_0 between synchronized and asynchronous condition

3.4 Dissipation of accumulated bending moment and variation of initial released angle

As mentioned in the section 9.1, in the synchronized condition, the time-dependent response of the bending moment at the tracking position (Θ=90°) was revealed as shown in Fig.11. When the hold time is kept in a certain duration, e.g. t_{1ep} >1s, the energy dissipation of accumulated bending moment seems to be characterized with the pre-stage folding velocity ω. As the result, when the release (returning back) process starts, the bending moment has a decreased level with respect to the pre-stage folding velocity ω.

Seeing Fig.13 and Fig.14, the initial release angle $\theta_{2,1}(0)$ increased with the velocity ω (in the synchronized condition) when t_{1ep} >2s. This is the same as that the spring back energy of folded posture decreases with ω when the hold time is

[DOI: 10.1299/jamdsm.2019jamdsm0004]

longer than 2s. Comparing this tendency with the variance of $M_{90,1}(t_{1ep})$, it is revealed that the pre-stage and the early stage of the hold time (e.g., $t_{1ep} < 1$ or 2s) are extremely sensitive to the relaxation or dissipation of accumulated bending moment energy. From the results of Fig.13, 14, and also seeing Fig.12 (b), the quasi-stationary relaxation of holding motion is performed for t_{1ep}>5s.

4. Conclusions

One-loop bending characteristics of creased white-paperboard of 0.3mm thickness were investigated by varying the folding rotational velocity ω and the unfolding (returning back) rotational velocity ω' when the hold time t_{1ep}= 0~20s was considered at the tracking position of Θ=90°, using a digital microscope camera. Through this work, the followings were found.

1) The release angle $\theta_{2,1}(t_{2ep})$ was characterized with a logarithmic function of the elapsed release time t_{2ep} for the measured range of t_{2ep}= 0~10s, when keeping the folding and unfolding rotational velocities in a constant. The release angle $\theta_{2,1}(t_{2ep})$ appears to be decomposed into the intercept part b_0 which is determined by the hold time t_{1ep} at the tracking position and the gradient part p_2 which is independently related to the release time t_{2ep}.
2) In the case of $\omega=\omega$'=0.2 rps (1.26 rad·s^{-1}), the exponential coefficient $p_2 = b_1/b_0$ of Eq.(4) was stably 0.050~0.053 for t_{1ep}= 0~20s, whereas the coefficients b_0, b_1 of E.(3) were limitedly saturated for t_{1ep} >5s.
3) When varying the folding and unfolding (released) rotational velocities under the synchronized condition: $\omega=\omega$' for $0.1 \leq \omega/0.2 \leq 3$, the initial release angle $\theta_{2,1}(0)$ was characterized with a logarithmic term $\ln(\omega/0.2)$ using the gradient coefficient $\beta_1 = \partial\theta_{2,1}(0) / \partial(\ln(\omega/0.2))$ and the intercept $\beta_0 = \theta_{2,1}(0)|_{\omega=0.2\text{rps}}$.
4) When t_{1ep}<2s, the coefficients β_1 and β_0 were remarkably varied. A change in the sign of β_1 occurred at this duration. When t_{1ep} >5s, β_1 and the ratio β_1/β_0 were asymptotically and slightly increased with t_{1ep}.
5) Regarding the response of bending moment, a drop rate of the bending moment in the early stage (t_{1ep}= 0~1s) of holding process remarkably increased with the term $\ln(\omega/0.2)$ for $0.1 \leq \omega/0.2 \leq 3$, whereas the relaxation behavior settled down with the exponential coefficient $p_1 = a_1/a_0$ of Eq.(2) for t_{1ep} >1s. Comparing this early stage of bending moment with the item 4), it was revealed that the gradient coefficient β_1 was under a transient state of the relaxation for t_{1ep}<2s, while that was under a quasi-stationary state for t_{1ep} >5s.
6) When varying the folding velocity ω under keeping the unfolding velocity ω'=0.2 rps (1.26 rad·s^{-1}) (asynchronous condition), the gradient coefficient β_1 and the ratio β_1/β_0 were relatively smaller than that of synchronized condition. Also, the value of β_1/β_0 was stably invariant for t_{1ep}>10s.
7) Seeing 3), 4) and 6), the hold time at the tracking position makes the folded part in relaxed state and then the holding posture isolates the second half unfolding released behavior from the first half folding rotational velocity effect when the hold time is longer than 5s.

Nomenclature

d : indentation depth of creaser knife
t : thickness of work sheet (paperboard)
B : width of groove on counter face plate
$\gamma = 2d \cdot B^{-1}$: normalized indentation depth, (γ = 0.6 was chosen in this work)
M : bending moment for the unit width against folding (Nm·m^{-1})
θ : folding angle of fixture (°)
Θ : tracking (maximum) angle (°) (Θ= 90° was chosen in this work)
n : number of folding repetitions (n=1 was considered in this work)
$M_{\Theta(,n)}$: the n-th round bending moment at a tracking position
$\theta_{1,n}$, $\theta_{2,n}$: the n-th round starting, release (angle) position ($\theta_{1,1}$ was zero in this work)
t_{1ep}: the n-th round hold time before returning back (t_{1ep} was varied from 0 up to 20s, in this work)
t_{2ep}: the n-th round elapsed release time until the next folding (t_{2ep} was measured up to 10s in this work)
ω : rotational velocity of fixture for folding (rps, revolution per second) (= $2\pi\omega$ rad·s^{-1})
ω' : rotational velocity of fixture for unfolding (released, returning back process) (rps) (= $2\pi\omega'$ rad·s^{-1})
a_1, a_0 : relaxation coefficients derived from Eq. (1) Here, a_0 is $M_{\Theta,1}$ at t_{1ep}=1s.
$p_1 = a_1 \cdot a_0^{-1}$: an exponential coefficient derived from Eq. (1), Eq.(2)
b_1, b_0 : release coefficients derived from Eq.(3) Here, b_0 is the intercept as $\theta_{2,1}$ at t_{2ep}=1s.

[DOI: 10.1299/jamdsm.2019jamdsm0004]

$p_2 = b_1 \cdot b_0^{-1}$: an exponential coefficient derived from Eq.(3), Eq.(4)
$\theta_{2,1}(0)$: initial release angle
β_1, β_0: gradient coefficient and intercept derived from Eq.(9) Here, $\beta_0 = \theta_{2,1}(0)|_{\omega=0.2\text{rps}}$

Acknowledgement

This work was supported by a fund for developing a core of excellence as innovative and branding project, from the GIGAKU Innovation Promotion Center, NUT, 2012-2016.

References

Beex, L.A.A, Peerlings, R.H.J., An experimental and computational study of laminated paperboard creasing and folding, International Journal of Solids and Structures, Vol.46, No.24, (2009), pp.4192-4207, DOI: 10.1016/j.ijsolstr. 2009.08.012.

Betten, J., Creep Mechanics, Springer (2002), pp.185-193.

CST-J-1, Katayama Steel Rule Die Inc., Tokyo, Japan (online), available from <diemex.com/sale/cst_e.html>, (accessed on May, 2013).

Hine, D.J., Testing boxboard creasing, Modern Packaging, Vol.8, (1959), pp. 122-128.

Johanson, F., Kubat, J., Measurements of Stress Relaxation in Paper, Svensk Papperstidning, Vol.20, No.31 (1964), pp.822-832.

Kirwan, M.J., Folding cartons (Handbook of Paper and Paperboard Packaging Technology), 2nd eds., M.J. Kirwan (Ed.), Wily-Blackwell (2013), pp.265-312.

Nagasawa, S., Fukuzawa, Y., Yamaguchi, T., Tsukatani, S. & Katayama, I., Effect of crease depth and crease deviation on folding deformation characteristics of coated paperboard, Journal of Materials Processing Technology, Vol.140, (2003), pp. 157-162, DOI: 10.1016/S0924-0136(03)00825-2.

Nagasawa, S. Murayama, M., Fukuzawa, Y. & Sadamoto, A., Mechanics of Die Cutting for Paperboard Materials Processing, 1st eds., Nagasawa (Ed.), Kameda book service (2004), pp.88-89.

Nagasawa, S., Endo, R., Fukuzawa, Y., Uchino, S. & Katayama, I., Creasing characteristic of aluminum foil coated paperboard, Journal of Materials Processing Technology, Vol.201, (2008), pp. 401–407, DOI: 10.1016/j.jmatprotec. 2007.11.253.

Nagasawa, S., Nasuruddin, M., Shiga, Y., Bending Moment Characteristics on Repeated Folding Motion of Coated Paperboard Scored by Round-Edge Knife, Journal of Advanced Mechanical Design, Systems, and Manufacturing, Vol.5, No.4, (2011), pp.385-394, DOI: 10.1299/jamdsm.5.385.

Nagasawa, S., Shiga, Y., Fukuzawa, Y., Effects of scoring depth, tracking angle, rubbering on bending-moment relaxation of creased paperboard, Advanced Materials Research, 939 (2014), pp.53-59, DOI: 10.4028/www.scientific.net/ AMR.939.53.

Nagasawa, S., Ozawa, S., Fukuzawa, Y., Effects of folding numbers, scoring depth and bending velocity on bending-moment relaxation of creased paperboard, Mechanical Engineering Journal, Vol.2 No.1, (2015), 14-00346, pp.1-9, DOI: 10.1299/mej.14-00346.

Nagasawa, S., Ozawa, S., Effect of bending velocity on time-dependent release behavior of creased white-coated paperboard, Mechanical Engineering Journal, Vol.3 No.3, (2016), 16-00182, pp.1-11, DOI: 10.1299/mej.16-00182.

Nagasawa, S., Adachi, D., Sasada, N., Effect of Stopping Time on Time-Dependent Release Behavior of Creased White-Coated Paperboard and Analysis of Nonlinear Relaxation Characteristics, Journal of the Japan Society for Technology of Plasticity (in Japanese), Vol.58 No.673 (2017), pp.151-156, DOI: 10.9773/sosei.58.151.

Nygards, M., Just, M., Tryding, J., Experimental and numerical studies of creasing of paperboard, International Journal of Solids and Structures, Vol.46, No.11-12, (2009), pp.2493-2505, DOI: 10.1016/j.ijsolstr.2009.02.014.

Sharon, K.W., Etienne, M., Efraim, L., Stress Relaxation of a Paper Sheet under Cyclic Load: An Experimental and Theoretical Model, Material Science and Application, Vol.1 (2010), pp.317-322, DOI: 10.4236/msa.2010.16046.

Sudo, A., Nagasawa, S., Fukuzawa, Y., Katayama, I., Analysis of exfolidation of laminated layers and creasing deformation of paperboard, Proceedings of the JSME HS annual meeting, No.047-1, (2005), pp.35-36 (in Japanese), DOI:10.1299/ jsmehs.2005.42.35.

